Journal of Marine Science and Technology

Volume 23 | Issue 4 Article 14

DEVELOPMENT AND PERFORMANCE OF AN ELECTRO-MAGNETIC DRIVEN MINIATURE PISTON PUMP

Han-Chieh Chiu
Department of Mechanical Engineering, Taipei Chengshih University of Science and Technology, Taipei , Taiwan

Chi-Hsiao Yeh
MD, Ph.D., Department of Thoracic and Cardiovascular Surgery, Chan Gung Memorial Hospital at Keelung, Keelung, Taiwan/College of Medicine, Chang Gung University, Tao-Yuan, Taiwan

Hung-Wei Yeh
Department of Mechanical Engineering, Taipei Chengshih University of Science and Technology, Taipei , Taiwan

Jer-Huan Jang
Department of Mechanical Engineering/Battery Research Center of Green Energy, Ming Chi University of Technology, New Taipei City, Taiwan, jhjang@mail.mcut.edu.tw

Follow this and additional works at: https://jmstt.ntou.edu.tw/journal

 Part of the Engineering Commons

Recommended Citation

Chiu, Han-Chieh; Yeh, Chi-Hsiao; Yeh, Hung-Wei; and Jang, Jer-Huan (2015) "DEVELOPMENT AND PERFORMANCE OF AN ELECTRO-MAGNETIC DRIVEN MINIATURE PISTON PUMP," *Journal of Marine Science and Technology*: Vol. 23: Iss. 4, Article 14.
DOI: 10.6119/JMST-015-0205-1
Available at: https://jmstt.ntou.edu.tw/journal/vol23/iss4/14

This Research Article is brought to you for free and open access by Journal of Marine Science and Technology. It has been accepted for inclusion in Journal of Marine Science and Technology by an authorized editor of Journal of Marine Science and Technology.

DEVELOPMENT AND PERFORMANCE OF AN ELECTRO-MAGNETIC DRIVEN MINIATURE PISTON PUMP

Acknowledgements

The authors would like to acknowledge the financial support of the present work by Chang Gung Memorial Hospital through projects CMRPG2B0511, CMRPG2B0521, CMRPG2B0531, and CMRPG2B0541. The authors are also grateful to Taipei Chengshih University of Technology for research support. Suggestions from Dr. Y. C. Chung are much appreciated as well.

This research article is available in Journal of Marine Science and Technology: https://jmstt.ntou.edu.tw/journal/vol23/iss4/14

Journal of Marine Science and Technology, Vol. 23, No. 4, pp. 508-515 (2015)
DOI: 10.6119/JMST-015-0205-1

DEVELOPMENT AND PERFORMANCE OF AN ELECTRO-MAGNETIC DRIVEN MINIATURE PISTON PUMP

Han-Chieh Chiu[1], Chi-Hsiao Yeh[2], Hung-Wei Yeh[1], and Jer-Huan Jang[3]

Key words: electro-magnetic driven motion, miniature pump, piston, performance.

ABSTRACT

An electro-magnetic driven miniature piston pump with novel mechanism has been developed for testing the feasibility in the present study. The novel mechanism is a hollowed piston in axial direction with a membrane served as a check valve. The operation of this novel pump is driven by electro-magnetic force to produce reciprocating motion with periodical switch of magnetic poles. The detailed operating principle is described for the magnetic driven reciprocating pump. The working fluid is water in this investigation. Our results include the performance and characteristics of the novel miniature pump. Testing results show that the maximum head is linearly proportional to the applied electric current. In addition, the relation between the head and flow rate is also close to linear, except for extreme conditions. The hydraulic efficiency and the volume efficiency were calculated to be close as 0.96 and 0.95, respectively.

I. INTRODUCTION

Miniature pumps have been applied to more areas with development of new technology in the past decades (Nbuyen and Werely, 2002). The applications include close-loop liquid cooling system in electronic device, circulating flow in direct methanol fuel cell, and medical dosing equipment (Jang and Kan, 2007; Ma et al., 2010). These applications require pumps with small size, low power consumption, and leakage free.

A conventional pump is normally composed of motor and shaft system that drive the impeller or piston inside the pump. It is difficult to reduce the system size due to complicated configuration. Besides, the seal between shaft and pump shell may leak after operating for a certain period of time. Various miniature pumps have been developed to fulfill specific applications. These include rotary pumps (Sen et al., 1996; Dopper et al., 1997; da Silva et al., 2007; Rossetti et al., 2010; Shin and Sung, 2010), piezoelectric pumps (Miyasaki et al., 1991; Olsson et al., 1995; Nguyen et al., 2001; Blanchard et al., 2005; Rossetti et al., 2009), thermo-pneumatic pumps (Grosjean and Tai, 1999), etc. In miniature rotary pumps, components are made in small size through precision fabrication. These pumps are still actuated through motor and shaft system. The speed of motor is high in order to produce satisfying liquid delivery rate.

Blanchard et al. (2005) developed a miniature rotary shaft pump with maximum flow rate of 64.9 ml/min and maximum pressure head of 2.1 kPa. Piezoelectric pumps utilize thin piezoelectric material to drive liquid flow in piping system. The pump is actuated with suitable electric voltage (normally higher than 100V) and frequency (higher than 50 Hz) to obtain small vibration of material in designated direction. Liquid can be transported through pumps with chamber arrangement or deformation phase lag of several piezoelectric discs. The small deformation of high frequency for piezoelectric materials causes liquid flowing in pumps. Although the frequency is high, piezoelectric pumps normally perform low flow rate due to the small deflection and pump chamber size. Nguyen et al. (2001) demonstrated a piezoelectric miniature pump using printed circuit board, which produced a maximum pumping head of 7.0 kPa and a maximum flow rate of 1.4 ml/min. During the measurement, high temperature was detected in the chamber for high frequency. Thermo-pneumatic pumps are actuated through thermal expansion of materials. Heating and cooling process of thermally expandable medium, filled in a cavity in thermo-Pneumatic pumps, induces pressure change and actuates a flexible or movable part of thermo-Pneumatic pumps, by turn drives liquid flow through the pump. Grosjean and Tai (1999) developed a thermo-pneumatic micro-pump with flow rate up to 6.3 μl/min. The

Paper submitted 8/26/13; revised 08/25/14; accepted 02/05/15. Author for correspondence: Prof. Jer-Huan Jang (e-mail: jhjang@mail.mcut.edu.tw).
[1] Department of Mechanical Engineering, Taipei Chengshih University of Science and Technology, Taipei , Taiwan, R.O.C.
[2] MD, Ph.D., Department of Thoracic and Cardiovascular Surgery, Chan Gung Memorial Hospital at Keelung, Keelung, Taiwan/College of Medicine, Chang Gung University, Tao-Yuan, Taiwan, R.O.C.
[3] Department of Mechanical Engineering/Battery Research Center of Green Energy, Ming Chi University of Technology, New Taipei City, Taiwan, R.O.C.

liquid delivery performance of most miniature pumps are limited by low flow rate, high voltage, noise, complicated structure, or leakage concern.

Electro-magnetic driven pumps have been considered one of the solutions for miniature fluid delivery system. With external components such as electro-magnetic coils, an internal movable part can be actuated through pump housing. Hu et al. (2002) presented a peristaltic pump, which was electro-magnetic driven. The pumping head (50 kPa) and flow rate (up to 25 ml/min) were both considerable. However, the whole system was weighed at 200 g due to the structure arrangement.

The main purpose of this research is to develop a novel mechanism with electro-magnetic principle for miniature pump and to verify the feasibility of this novel pump with measurements of its performance and characteristics. The pump is able to perform considerable flow rate and pressure head with low power consumption, low voltage, simple configuration, and without leakage concern. Besides, it is light-weighted with compact size. The design utilizes electro-magnetic components outside the pump chamber to drive a piston inside. The piston is hollowed along the axial direction to form a channel which liquid can flow through. By suitable arrangement of membrane check valves, liquid can be delivered one-way through the pump.

II. PUMP CONFIGURATION AND ACTUATION

The configuration of the pump is composed of a shell/cylinder, an inlet, an outlet, two electromagnetic coils, and a piston (Fig. 1(a)). The major part of the pump (except the magnets and check valves) is computer numerical control machined with acrylic for easy fabrication, low weight, and motion observation. The piston is hollowed in the axial direction to form a flow channel that liquid can be delivered through. Two Nd-Fe-B sintered magnets (commercially made) are attached on both ends of the piston. The intrinsic coercivity of the magnets is 8.7×10^5 A/m. Both the piston and magnets are 5.0 mm in the outer diameter and 1.5 mm in the inner diameter. All the finished parts were then assembled together as shown in Fig. 1(b). The total weight of the piston assembly (including the magnets and the check valve) is 1.03 g. The lengths of the cylinder and the piston assembly are 25 mm and 22.5 mm respectively, giving a stroke length of 2.5 mm. In each cycle, the distance between the magnet and electromagnetic coil is varied between 3.5 mm and 1 mm. The inner diameter of the cylinder is 5.1 mm, leaving a clearance of 0.05 mm between the piston and cylinder. This clearance provides the piston to move freely inside the cylinder while allowing a thin film of the transported fluid to form between the piston and cylinder, which offers lubrication for these two parts. Two membrane check valves are installed on outlet end of the piston and the inlet of the pump respectively to prevent reverse flow. The electro-magnetic coils are made by winding

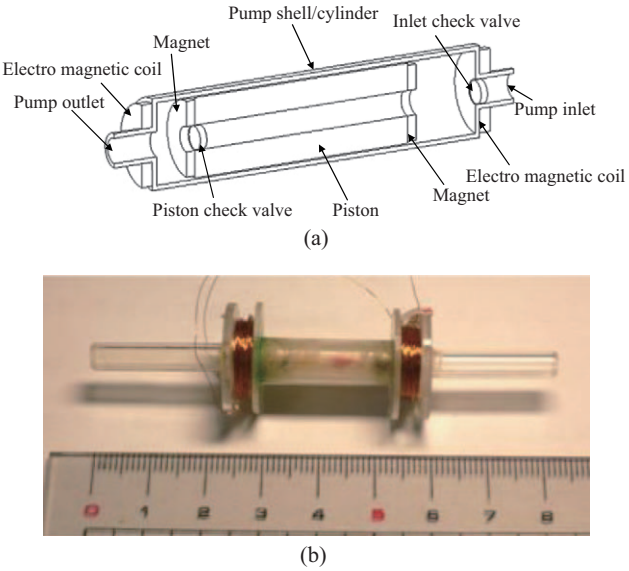

Fig. 1. (a) The configuration of the pump; (b) prototype.

enamel-insulated copper wire 0.14 mm in diameter with 400 ± 10 rounds, mounted on both ends of the shell/cylinder in parallel. The magnetic poles of the electro-magnetic coils can be switched by changing direction of the applied current. With proper control of the electric current and the arrangement of the magnetic force between the coils and the magnets on both ends of the piston, the piston is able to reciprocate continuously in the shell/cylinder. The actuation of piston is non-intrusive, neither motor nor shaft system through the pump shell is necessary. Hence the pump can be totally sealed, and leakage due to the shaft sealing can be eliminated completely. This simple configuration also provides advantages that it can be easily miniaturized and built with various cross sectional shapes.

The actuation of the piston can be described with two processes – the transport and intake-discharge process, shown in Fig. 2. During the transport process (Fig. 2(a)), magnetic fields are generated by the input current on both electromagnetic coils such that the same poles are facing each other between the coil and the magnet on the pump outlet side; while on the pump inlet side the opposite poles are facing each other between the coil and the magnet. With this arrangement, a repelling force between the coil and the magnet on the pump outlet side and an attracting force between the coil and the magnet on the pump inlet side are generated. The resultant force drives the piston assembly to move toward the inlet of the pump. The chamber on the inlet side is reduced, while the chamber on the outlet side is enlarged. In this process, the inlet membrane check valve is closed to prevent reverse flow, and the piston membrane check valve is opened, allowing liquid in the chamber on the inlet side to flow into the chamber on the outlet side. During the intake-discharge process (Fig. 2(b)), as the current is switched into the opposite direction, the magnetic fields generated on both electro-magnetic coils are

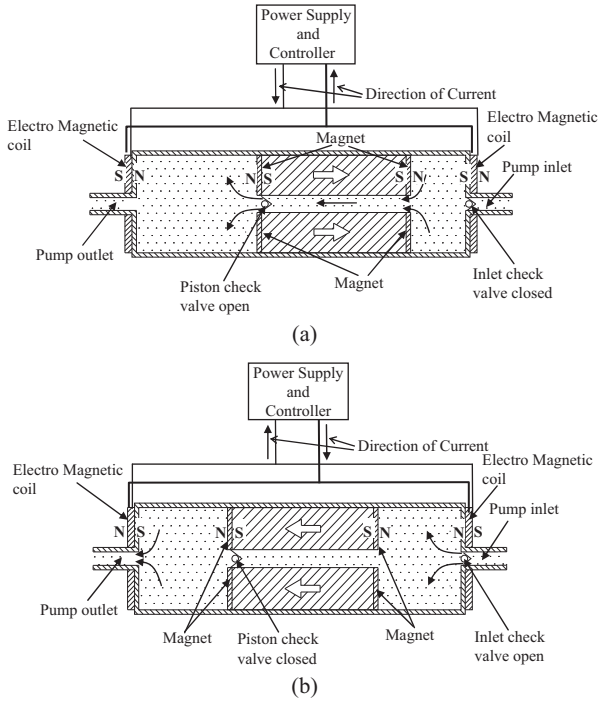

Fig. 2. The actuation of the pump in (a) the transport process, and (b) the intake-discharge process.

also switched into the opposite direction such that the opposite poles are facing each other between the coil and the magnet on the pump outlet side; while on the pump inlet side the same poles are facing each other between the coil and the magnet. With this arrangement, an attracting force between the coil and the magnet on the pump outlet side and a repelling force between the coil and the magnet on the pump inlet side are generated. The resultant force drives the magnets-piston assembly to move toward the outlet of the pump. As a result, the chamber on the outlet side is reduced, while the chamber on the inlet side is enlarged. During this process, the piston membrane check valve is closed, pushes liquid out of the pump through the outlet, while the inlet membrane check valve is opened, and liquid is drawn into the enlarging chamber on the inlet side. The continuous switching of the current direction creates repeating cycles of these two processes, results in liquid delivery through the pump.

III. THEORY OF OPERATION

Parameters that characterize pump performance include elevated head, volumetric flow rate, and hydraulic efficiency. During a typical operating cycle, the theoretical volumetric flow rate is proportional to the length of the stroke and the reciprocating frequency of the piston. Therefore, Q_{th} can be expressed as

$$Q_{th} = fAl \tag{1}$$

where f is the reciprocating frequency of the piston, A is the cross-sectional area of the cylinder, and l is the stroke length. The actual volume flow rate Q_{act} can be expressed as

$$Q_{act} = Q_{th} - Q_{loss} \tag{2}$$

where Q_{loss} is the loss flow rate which may come from reverse flow through the gap between the piston and the cylinder wall and membrane motion. The loss of the flow rate is also influenced by incomplete movement of the piston in a stroke. Therefore, the volume efficiency is defined as

$$\eta_V = \frac{Q_{act}}{Q_{th}} \tag{3}$$

The hydraulic efficiency (Miyasaki et al., 1991) can be written as

$$\eta_h = \frac{h}{h_{th}} \tag{4}$$

where h_{th} is the theoretical elevated head and h is the actual pumping head. The value of h_{th} can be estimated from $F_{p,\,max}/\gamma A$, where $F_{p,\,max}$ is the measured maximum value of magnetic force F_p during reciprocation of the piston, γ is the specific weight of liquid, and A is the cross section area of the piston.

In a reciprocating cycle, the work transported into liquid through piston can be expressed as $\int Fvdt$, where F is the net force exerted on the piston, and v is the moving velocity of the piston. The time domain of the integration is considered to be within the half cycle of forward motion since only this part of motion pushes water. The energy obtained by the liquid through flowing upward is expressed as $Q_{act}\gamma h/f$. The dynamic efficiency can be determined as

$$\eta_d = \frac{Q_{act}\gamma h}{f\int Fvdt} \tag{5}$$

Due to the complexity of relationship between F and v, the integral in Eq. (5) is approximated as the product of the averaged force, $\bar{F}$, and the stroke length in a cycle, l. Hence the dynamic efficiency can be approximately estimated as

$$\eta_d = \frac{Q_{act}\gamma h}{f\bar{F}l} \tag{6}$$

The physical meaning of dynamic efficiency represents an indication of the dynamic performance of the piston rather than the pump efficiency. The theoretical shut-off head of the pump, h_{sh}, is defined as the maximum force exerted on the piston divided by the piston cross-section area. The pumping head h during operation can be normalized as

$$h^* = \frac{h}{h_{sh}} \tag{7}$$

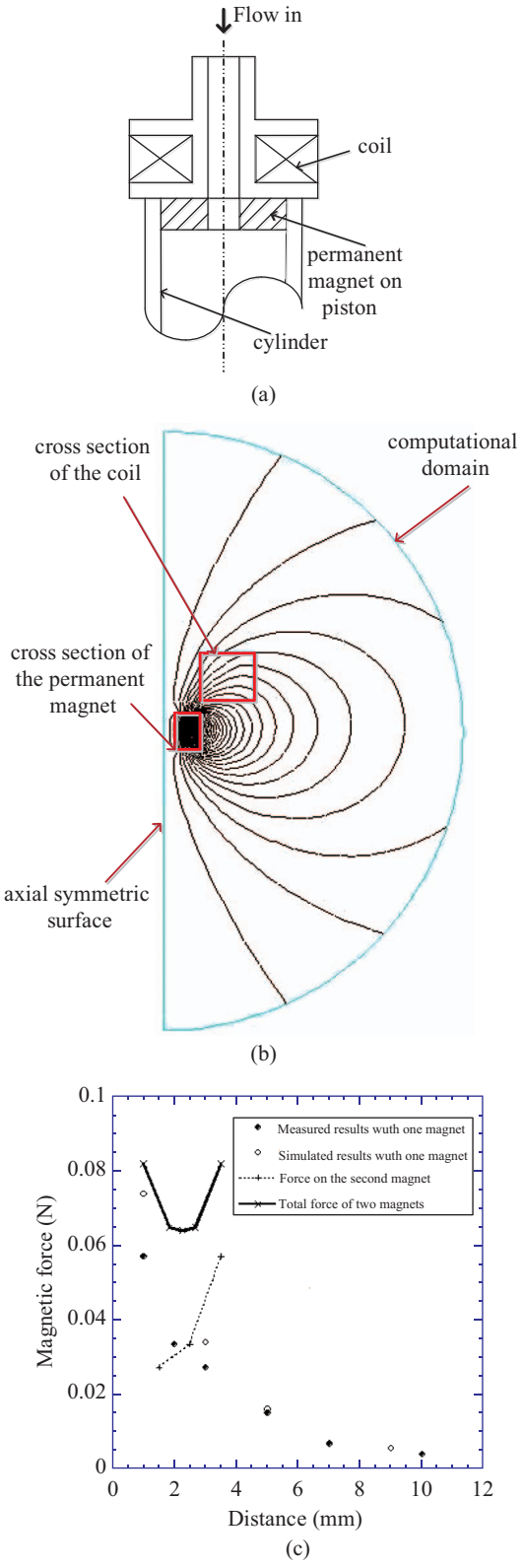

Fig. 3. (a) schematic illustration for analysis; (b) The magnetic field from ANSYS simulation; (c) The relation of electro magnetic force and magnetic flux distance. The discrete data are measured force as a function of the distance between a magnet surface and a coil. The dashed line is the estimated force exerted on the opposite magnet. The solid line is the total force of the two magnets.

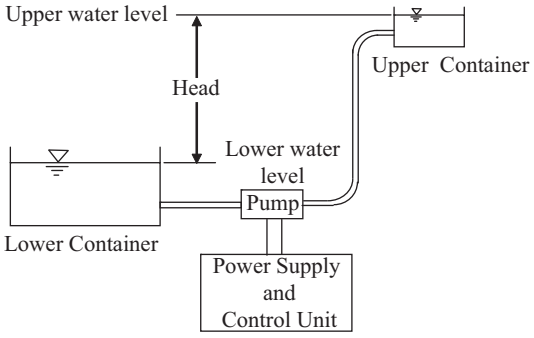

Fig. 4. The schematic of test setup.

IV. EXPERIMENTAL APPARATUS AND PROCEDURES

1. Determination of Magnetic Force on the Piston

In order to estimate the force exerted on the piston during a stroke, the force of an electro-magnetic coil exerted on a magnet has been measured. The magnetic force was also estimated with ANSYS simulation for comparison with experimental results. The measurement was conducted with magnet placed on an electronic scale, while a coil with 0.2A current moved close to the magnet. The coil was originally held 15.0 mm above the magnet with the same magnetic poles facing each other, producing repelling force on the scale. The coil was then moved vertically toward the magnet, and the magnitude of the force shown on the scale was recorded with respect to the distance (Fig. 3(c)). Since the magnetic attracting and repelling force were exerted on the piston at the same time, at any moment during the motion of the piston the total force on the piston was the sum of these two forces and could be found as superposition of the two data curves. The schematic illustration of the magnetic field of the pump for axial distance of 1.0 mm between permanent magnet and coil is shown in Fig. 3(a). Fig. 3(b) depicts result of the magnetic field of the pump from ANSYS simulation. Since the axial view of the geometry is axis-symmetric, the simulation is made with cross section. The smaller rectangle on the left is the cross section of the permanent magnet, and the larger rectangle is the cross section of the coil. The vertical line represents the symmetric line. The outer half circle represents infinite boundary of the magnetic field. The mesh element number was set in the range of 1500~1800. Double element number resulted in difference less than 3%. Hence the mesh resolution is considered enough. The simulated results of the magnetic repelling force are close to the measured results in Fig. 3(a). The deviation may be due to material non-uniformity or geometry difference between the model and the real coil. The attractive force and repelling force from simulation are found to be the same for same distance. Therefore measurement of the repelling force is sufficient for this study.

2. Setup of Experimental Apparatus

The test setup is shown in Fig. 4. The pump was connected

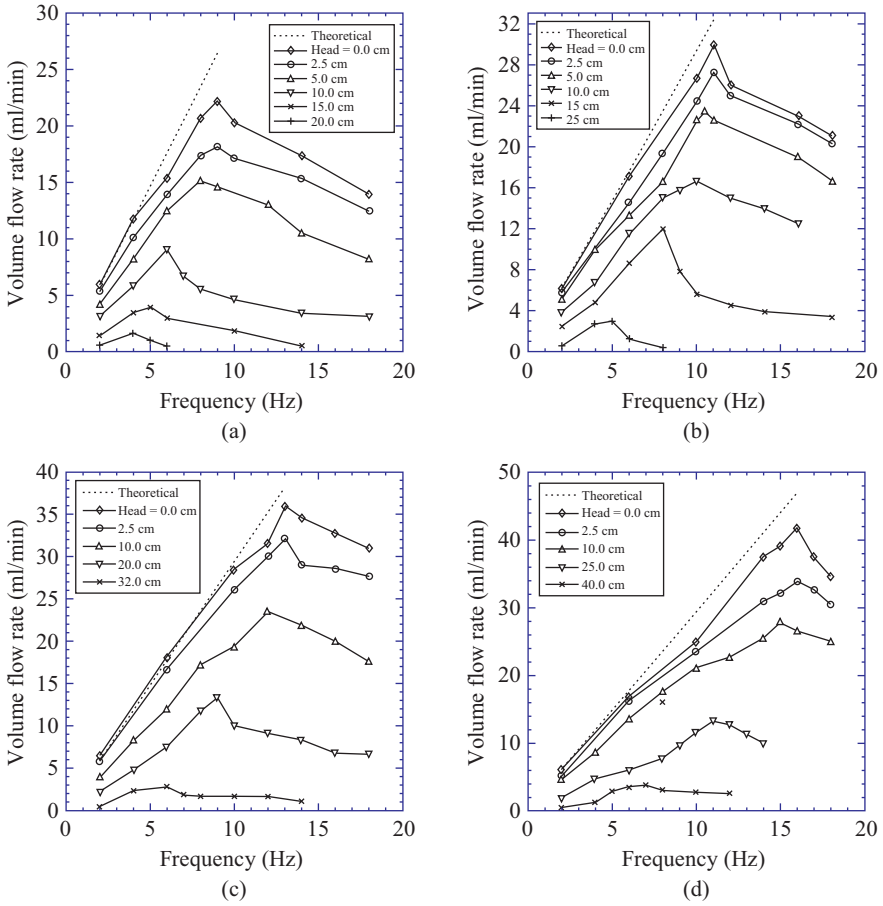

Fig. 5. Volume flow rate for various pumping heads with applied electric current of (a) 0.2A, (b) 0.3A, (c) 0.4A, and (d) 0.5A. The dashed line is the estimated flow rate under ideal condition.

to two water containers at different levels. The electromagnetic coils on the pump were connected to frequency control unit and a power supply unit. The frequency control unit periodically switched the direction of the electric current, causing the magnetic force acting on the piston to reciprocate back and forth. The lower container connected to the left end of the pump was about 280 cm^2 in cross section area such that the change of water level during water delivery could be neglected. The upper container was connected to the right end of the pump with a free surface setting at a specified head, which is the difference in height between the two free surfaces of the lower and upper containers. The water in the lower container was pumped into the upper container and overflowed to a measuring device, keeping the free surface at a constant level. On the other hand, the flow rate can be determined by recording the time required for a certain increment of volume inside the measuring device.

3. Procedures of Measurements

i. Set the current at 0.20A. In turn, there is 0.10A through each of the two parallel coils.
ii. Set the difference of the water levels between two containers as zero.
iii. The frequency was set as a variable ranging from 2.0 to 12.0 Hz. At each frequency, the time required for pumping specified volume of water was recorded. The volume flow rate can then be estimated.
iv. Adjust the difference of the water levels between two containers (head) by raising the upper container to specified heights. For each specified head h, repeat step iii and record the flow rate as a function of frequency.
v. Raise the current to 0.3, 0.4, and 0.5A. At each current, repeat steps ii through iv, and record the results. This pump can be operated under 3V when the current is 0.3A. The total power consumption is less than 1W for current 0.3A.

V. RESULTS AND DISCUSSIONS

In Fig. 5, the flow rate Q_{act} is plotted against the reciprocating frequency at specified elevated heads for current of 0.2, 0.3, 0.4, and 0.5A, respectively. The theoretical flow rate Q_{th} with respected to frequency f is also presented as a dashed line for comparison. The results show that for a specified elevated head, there exists an optimal flow rate Q_o and a corresponding frequency f_o. At lower frequency ($f < f_o$), the flow

rate is almost linearly proportional to the frequency; while at higher frequency ($f > f_o$), the flow rate decays non-linearly with increasing frequency. During the experiment, it was observed that the piston reached both ends of the cylinder in each cycle at frequencies lower than f_o. Hence during the intake-discharge process, the front end of the piston reached the outlet end of the cylinder, and during the transport process the piston reached the inlet end of the cylinder at each stroke. Since the stroke length is a constant in this frequency range, the volume flow rate is dependent on the frequency as shown in Eq. (1). However, it is clear that there is a deviation for measured data with theoretical values. Also, it is noted that the deviation increases with increasing head. When the frequency is greater than f_o, the motion of the piston no longer reaches both ends of the cylinder, and the flow rate decreases due to incomplete movement of the piston and lower pumping efficiency. Similar characteristics were observed for all heads. The Q_{loss} is significant for a higher head due to more severe reverse flow when frequency is less than f_o. In addition, as frequency is greater than f_o, the Q_{loss} is majorly attributed to incomplete movement of piston in a stroke. It is of interest to see that the value of f_o decreases with increasing head. This is probably due to the lower net force on the piston. The effects of the applied current on the performance characteristics of the pump can be observed in Fig. 5. In comparison of each figure for the same head, it is seen the optimal flow rate Q_o increases with increasing current, so does the corresponding optimal frequency f_o. For zero-head situation, i.e., f_o is raised from 9 Hz to 16 Hz when the current is increased from 0.2A to 0.5A. Because the increase in electro-magnetic force transports more energy into the fluid, resulting in faster piston motion and higher flow rate.

At higher elevated heads for each current setting, the data show almost no flow rate at frequency less than 2 Hz. Under such situation, the amount of water pumped out per second at each stroke was annihilated by the amount of Q_{loss}, making the net out flow rate close to zero. In addition, the check valves for both inlet and outlet do not fit perfectly, making contribution to Q_{loss} for high head and frequency below 2 Hz. On the other hand, due to the slow motion, when the piston moved forward away from the pump inlet, the intake chamber was quickly filled up by the reverse flow, and the opening of the inlet membrane valve was suppressed. The water flow can only circulated inside the pump. Once the frequency is increased, the out flow rate starts to increase gradually over Q_{loss}, and the net flow out of the pump is resumed. This explains why certain low reciprocating frequency would result in no liquid flow of the pump. Therefore, the experimental data with frequency lower than 2 Hz are not shown in the figures.

Fig. 6 presents the relation between head and optimal flow rate Q_o with various currents. It is noted that the curves are different from those of traditional pumps, which are parabolic curves. It is shown that Q_o and h are almost inversely linear proportional to each other in the middle range of the curves. According to Eq. (2), the actual flow rate is determined by the

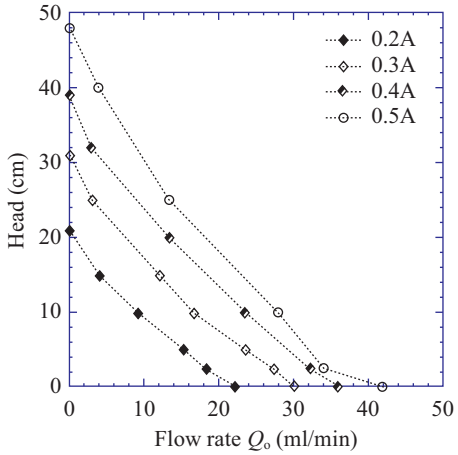

Fig. 6. The relation between pumping head and corresponding optimal flow rate with various applied electric current.

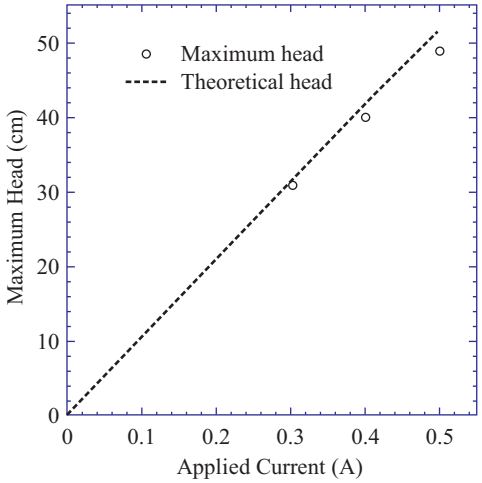

Fig. 7. The maximum head with respect to applied electric current.

difference between Q_{th} and Q_{loss}. It is interesting to see that the slope at lower Q (higher head) tends to rise up. At very high head, the amount of Q_{loss} becomes close to Q_{th} in each cycle. Although the piston is still reciprocating, the water only circulates within the chambers formed by the motion of the piston, and the flow rate becomes close to zero. The head without flow rate is defined as the maximum head h_{max}. Comparison of the curves indicates that increasing current results in more augmentation in h_{max} than that in the zero-head flow rate.

Fig. 7 depicts the maximum head h_{max} as a function of the applied current. The dashed line is the theoretical shut-off head h_{sh} as a function of applied current. The measured value of h_{max} is almost linearly proportional to the applied current. The slight discrepancies between the theoretical h_{sh} and the measured h_{max} at higher currents are due to the reverse flow at high head. As the h_{sh} increases with higher input current, the static pressure of the fluid also grew higher. This higher pressure not only causes higher resistance to the piston during the

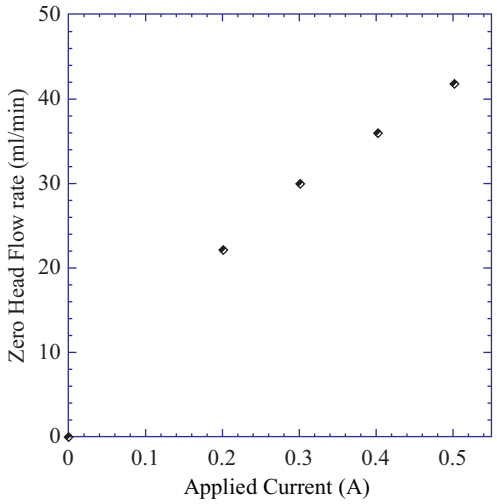

Fig. 8. The relation between free delivery flow rate and applied electric current.

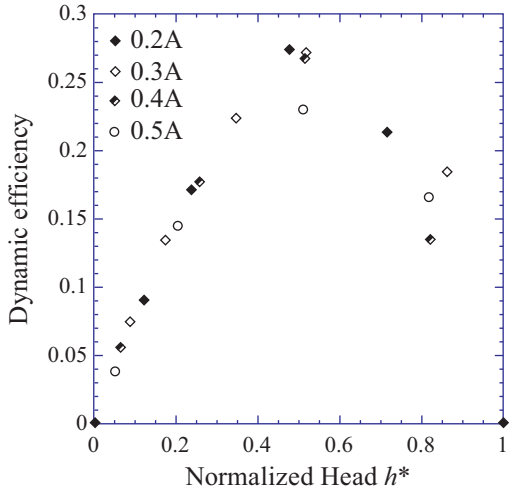

Fig. 9. Dynamic efficiency with respect to normalized head.

intake-discharge step but also tends to increase Q_{loss}. This loss made the measured h_{max} lower than the corresponding theoretical value. The situation becomes more severe for higher h_{sh}, shown as the increasing discrepancy from 0.4A to 0.5A. The hydraulic efficiency is calculated to be 0.92~0.96 for different currents. The zero-head optimal flow rate is plotted as a function of the applied current in Fig. 8. It is observed that zero-head optimal flow rate increases with the increasing applied current. However, the slope decreases with increasing current. The corresponding f_o for each data point is not the same as aforementioned. According to Eqs. (1) and (3), the volume efficiency η_V is calculated to be 0.88~0.95 for various currents.

Fig. 9 presents the functional relation between the dynamic efficiency and the normalized head. All the curves for different currents are close to each other, showing similar to the parabolic function with the maximum values close to 0.30. The optimal pump performance appears with h^* in the range between 0.52 and 0.58. The pump for the present study is a prototype for feasibility. Further work on optimizations surely will improve the performance of this pump.

VI. CONCLUSION

In this study, the performance of a novel mechanism with electro-magnetic driven miniature piston pump is presented. The results show the feasibility for low power consumption and leakage free configuration. The performance curves for various input currents have similar characteristics. Such behavior is different from those of traditional pumps. The measured maximum head is almost linearly proportional to the applied current. For the tested conditions, a maximum head as high as 48 cm and a maximum flow rate of 42 ml/min are achieved with input electric current of 0.5A and potential of 5V. The hydraulic efficiency and the volume efficiency have been estimated to be as high as 0.96 and 0.95, respectively. The dynamic efficiency shows optimal operation range of 0.52~0.58 normalized head. Further study on pump configurations and electro-magnetic parts can be conducted to improve the pump performance.

ACKNOWLEDGMENTS

The authors would like to acknowledge the financial support of the present work by Chang Gung Memorial Hospital through projects CMRPG2B0511, CMRPG2B0521, CMRPG2B0531, and CMRPG2B0541. The authors are also grateful to Taipei Chengshih University of Technology for research support. Suggestions from Dr. Y. C. Chung are much appreciated as well.

REFERENCES

Blanchard, D., P. Ligrani and B. Gale (2005). Performance and development of a miniature rotary shaft pump. ASME J. Fluids Engineering 127, 752-760.

da Silva, A. K., M. H. Kobayashi and C. F. M. Coimbra (2007). Optimal theoretical design of 2-D microscale viscous pumps for maximum mass flow rate and minimum power consumption. International Journal of Heat and Fluid Flow 28(3), 526-536.

Dopper, J., M. Clemens, W. Ehrfeld, S. Jung and K.-P. Kamper (1997). Micro gear pumps for dosing viscous fluids. J. Micromech. Microeng. 7, 230-232.

Grosjean, C. and Y.-C. Tai (1999) A thermopneumatic peristaltic micropump. Proceedings of the International Conference on Solid-State Sensors and Actuators (Transducers '99), Sendai, Japan, 1776-1779.

Hu, M., H. J. Du and S. F. Ling (2002). A digital miniature pump for medical applications. IEEE/ASME Transaction on Mechatronics 7(4), 519-523.

Jang, L. S. and W. H. Kan (2007). Peristaltic piezoelectric micropump system for biomedical application. Biomed Microdevices 9(4), 619-626.

Ma, Y. T., F. R. Kong, C. L. Pan, Q. Zhang and H. F. Feng (2010). Miniature tubular centrifugal piezoelectric pump utilizing wobbling motion. Sensors and Actuators A 157, 322-327.

Miyasaki, S., T. Kawai and M. Araragi (1991). A piezoelectric pump driven by a flexural progressive Wave. Proc. of MEMS'91, 4th Int. Workshop MEMS, Nara, Japan, 199-202.

Nbuyen, N.-T. and S. T. Werely (2002). Fundamentals and Applications of Microfluidics, Artech House, Norwood, 292-337.

Nguyen, N.T. and X. Y. Huang (2001). Miniature valveless pumps based on printed circuit board techniques. Sens. Actuators 88(2), 104-111.

Olsson, A., G. Steeme and E. Steeme (1995). A valve-less planar fluid pump with two pump chambers. Sens. Actuators A47(2), 549-556.

Rossetti, A., G. Pavesi and G. Ardizzon (2009). Experimental and numerical analyses of micro rotary shaft pumps. J. Micromech. Microeng 19(12), 125013.

Rossetti, A., G. Pavesi and G. Ardizzon (2010). A new two stage miniature pump: Design, experimental characterization and numerical analyses. Sensors and Actuators A164(1-2), 74-87.

Sen, M., D. Wajerski and M. Gad-el-Hak (1996). A novel pump for MEMS application. ASME, J. Fluids Eng. 125(2), 339-344.

Shin, S. J. and H. J. Sung (2010). Three-dimensional simulation of a valveless pump. International Journal of Heat and Fluid Flow 31(5), 942-951.